Asymmetric control achieves size-independent stability margin in 1-D flocks

He Hao and Prabir Barooah

***Abstract*— We consider the stability margin of a large 1-D flock of double-integrator agents with distributed control, in which the control at each agent depends on the relative information from its nearest neighbors. In [1], it was shown that with symmetric control, in which two neighbors put equal weight on information received from each other, the stability margin of the flock decays to 0 as $O(1/N^2)$, where N is the number of agents. Moreover, a perturbation analysis was used to show that with vanishingly small amount of asymmetry in the control gains, the stability margin can be improved to $O(1/N)$. In this paper, we show that, in fact, with asymmetric control the stability margin of the closed-loop can be bounded away from zero uniformly in N. Asymmetry in control gains thus makes the control architecture highly scalable. In addition, an error analysis is provided to characterize the error introduced by using partial differential equation to approximate the dynamics of a large 1-D flock that used in [1]. We show that the PDE approximation is only valid for small amount of asymmetry. Numerical verifications are also provided to corroborate our analysis.**

I. Introduction

The problem of distributed control of multiple agents is relevant to many applications such as automated highway system, collective behavior of bird flocks and animal swarms, and formation flying of unmanned aerial and ground vehicles for surveillance, reconnaissance and rescue, etc. [2], [3], [4], [5]. A classical problem in this area is the distributed formation control of a 1-D flock of agents, in which each agent is modeled as a double integrator. The control action at each agent is based on the information from its two nearest neighbors (one on either side). The control objective is to make the flock track a desired trajectory while maintaining a rigid formation geometry. The desired trajectory of the entire formation is given in terms of a fictitious reference agent, and the desired formation geometry is specified in terms of constant inter-agent spacings.

A typical issue faced in this problem is that the performance of the closed-loop degrades as the number of agents increases. Several recent papers have studied the scaling of performance of formations of double-integrator agents as a function of the number of agents. In particular, [1], [6] have studied the scaling of the stability margin, while [7], [8], [9], [10] have examined the sensitivity to external disturbances. However, most of the work impose the condition that the information graph is undirected (i.e., symmetric), which means that between two agents i and j that exchange information, the weight placed by i on the information received from j is the same as the weight placed by j on that received from i. In a previous paper [1], it was shown that with symmetric control, the stability margin of the 1-D flock, which is measured by the real part of the least stable eigenvalue of the closed-loop, decays to 0 as $O(1/N^2)$, where N is the number of agents. The loss of stability margin with symmetric control has also been recognized by other researchers [9], [11].

In this paper, we study the stability margin of a large 1-D flock of double-integrator agents whose information graph is directed or asymmetric. Little work has been done on coordination of double integrator agents with directed information graphs, with [1], [10] being exceptions. It was shown in [1] that with vanishingly small asymmetry in the control gains, the stability margin can be improved to $O(1/N)$. Similar conclusions are also obtained for a vehicular formation with a D-dimensional lattice as its information graph [6]. The analyses in [1], [6] were based on a partial differential equation (PDE) approximation of the closed-loop dynamics and a perturbation method; the latter limited the results to only vanishingly small asymmetry. The reference [10] studied the effect of asymmetry in control on the flock's sensitivity to disturbances, but not its stability margin.

In this paper, we show that with a fixed amount of asymmetry in the control gains, the stability margin of the flock can be uniformly bounded away from 0 (independent of N). This stronger result - compared to those in [1], [6] – is obtained by avoiding the perturbation analysis of the aforementioned papers. We provide two alternate proofs of the result. One line of analysis proceeds with the PDE-approximation of the coupled-ODE model that was used in [1], [6]. Techniques from Strum-Liouville theory are used to derive a closed-form expression for the lower bound, which is then used to establish that the lower bound is independent of N. The second line of analysis deals with the coupled-ODE model directly. We also show that the prediction from the PDE analysis approaches the prediction from the coupled-ODE model as $\epsilon \to 0$, where ϵ quantifies the amount of asymmetry. Thus, the conclusions obtained from the PDE analysis are valid only for small amount of asymmetry. The advantage of the PDE-based analysis is that it provides powerful insights on the benefits of asymmetric control on the performance of the system, while the coupled-ODE model provides no insight into what kind of asymmetry may be beneficial.

We also show that the smallest eigenvalue of the *directed grounded Laplacian* of the information graph plays a pivotal role in determining the stability margin of the system. Al-

He Hao and Prabir Barooah are with Department of Mechanical and Aerospace Engineering, University of Florida, Gainesville, FL 32611, USA.
This work was supported by the National Science Foundation through Grant CNS-0931885 and ECCS-0925534, and by the Institute for Collaborative Biotechnologies through grant DAAD19-03-D-0004.

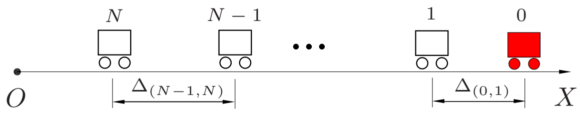

Fig. 1. Desired geometry of a flock with N agent and 1 "reference agent", which are moving in 1D Euclidean space. The filled agent in the front of the flock represents the reference agent, it is denoted by "0".

though our study is focused on agents with double integrator dynamics, eigenvalues of digraphs are also important in the study of convergence rate of distributed consensus, which is essentially coordination of vehicles with single-integrator dynamics. Even in the consensus literature, study of the graph Laplacian spectra for directed graphs has been rather limited [12]. In this paper we provide a formula for the smallest eigenvalues of the directed grounded Laplacian matrix for a 1-D lattice as a function of N. In addition, our results show the connection between the smallest eigenvalues of the directed grounded Laplacian matrix and a Strum-Liouville operator.

The rest of this paper is organized as follows. Section II presents the problem statement and main results. The stability margin of the flock with coupled-ODE model and its relationship with the smallest eigenvalue of its directed grounded Laplacian are stated in Section III. PDE-based analysis of stability margin and its approximation error appear in Section IV. The paper ends with a summary in Section V.

II. Problem Statement and Main Results

A. Problem statement

In this paper we consider the formation control of N identical agents which are moving in 1-D Euclidean space, as shown in Figure 1. The position of the i-th agent is denoted by $p_i \in \mathbb{R}$ and the dynamics of each agent are modeled as a double integrator:

$$\ddot{p}_i = u_i, \quad i \in \{1, 2, \cdots, N\}, \tag{1}$$

where $u_i \in \mathbb{R}$ is the control input, which is the acceleration or deceleration command.

The control objective is that the flock maintains a desired formation geometry while following a constant-velocity type desired trajectory. The desired geometry of the formation is specified by the *desired gaps* $\Delta_{(i-1,i)}$ for $i \in \{1, \cdots, N\}$, where $\Delta_{(i-1,i)}$ is the desired value of $p_{i-1}(t) - p_i(t)$. The desired inter-agent gaps $\Delta_{(i-1,i)}$'s are positive constants and they have to be specified in a mutually consistent fashion, i.e. $\Delta_{(i,k)} = \Delta_{(i,j)} + \Delta_{(j,k)}$ for every triple (i, j, k) where $i \le j \le k$. The desired trajectory of the flock is provided in terms of a *fictitious* reference agent with index "0", whose trajectory is denoted by $p_0^*(t)$. The information on the desired trajectory of the flock is only provided to agent 1. The desired trajectory of the i-th agent, $p_i^*(t)$, is given by $p_i^*(t) = p_0^*(t) - \Delta_{(0,i)} = p_0^*(t) - \sum_{j=1}^{i} \Delta_{(j-1,j)}$.

We consider the following *decentralized* control law used in [1], whereby the control action at the i-th agent depends on the relative position measurements with its nearest neighbors in the flock (one on either side), its own velocity, and the desired velocity v^* of the flock:

$$\begin{aligned} u_i = &- k_i^f (p_i - p_{i-1} + \Delta_{(i-1,i)}) - k_i^b (p_i - p_{i+1} - \Delta_{(i,i+1)}) \\ &- b_i (\dot{p}_i - v^*), \end{aligned} \tag{2}$$

where $i \in \{1, \cdots, N-1\}$, k_i^f, k_i^b are the front and back position gains and b_i is the velocity gain of the i-th agent. For the agent with index N, the control law is given by:

$$u_N = -k_N^f (p_N - p_{N-1} + \Delta_{(N-1,N)}) - b_N (\dot{p}_N - v^*), \tag{3}$$

since it does not have a neighbor behind it. Each agent i knows the desired gaps $\Delta_{(i-1,i)}$, $\Delta_{(i,i+1)}$, while only agent 1 knows the desired trajectory $p_0^*(t)$ of the fictitious reference agent. To facilitate analysis, we define the tracking error:

$$\tilde{p}_i := p_i - p_i^* \qquad \Rightarrow \qquad \dot{\tilde{p}}_i = \dot{p}_i - \dot{p}_i^*. \tag{4}$$

The closed-loop dynamics can now be expressed as the following coupled-ODE model

$$\begin{aligned} \ddot{\tilde{p}}_i &= -k_i^f (\tilde{p}_i - \tilde{p}_{i-1}) - k_i^b (\tilde{p}_i - \tilde{p}_{i+1}) - b_i \dot{\tilde{p}}_i, \\ \ddot{\tilde{p}}_N &= -k_N^f (\tilde{p}_N - \tilde{p}_{N-1}) - b_N \dot{\tilde{p}}_N. \end{aligned} \tag{5}$$

where $i \in \{1, \cdots, N-1\}$, which can be represented in the following state-space form:

$$\dot{x} = Ax, \tag{6}$$

where $x := [\tilde{p}_1, \dot{\tilde{p}}_1, \cdots, \tilde{p}_N, \dot{\tilde{p}}_N] \in \mathbb{R}^{2N}$ is the state vector.

In [1], a PDE was derived as an approximation of the coupled-ODE model (5) for large N. The PDE governed the evolution of $\tilde{p}(x,t) : [0,1] \times \mathbb{R}_+ \to \mathbb{R}$, which is a spatially continuous counterpart of the functions $\tilde{p}_i(t)$, $i \in \{1, \cdots, N\}$, with the stipulation that $\tilde{p}_i(t) = \tilde{p}(x,t)|_{x=(N-i)/N}$. The PDE model is given by

$$\begin{aligned} \frac{\partial^2 \tilde{p}(x,t)}{\partial t^2} + b(x) \frac{\partial \tilde{p}(x,t)}{\partial t} = &\frac{k^f(x) - k^b(x)}{N} \frac{\partial \tilde{p}(x,t)}{\partial x} \\ &+ \frac{k^f(x) + k^b(x)}{2N^2} \frac{\partial^2 \tilde{p}(x,t)}{\partial x^2}, \end{aligned} \tag{7}$$

with mixed Dirichlet-Neumann boundary condition

$$\frac{\partial \tilde{p}}{\partial x}(0,t) = 0, \qquad \tilde{p}(1,t) = 0, \tag{8}$$

where $k^f(x), k^b(x), b(x) : [0,1] \to \mathbb{R}_+$ are the continuous approximations of the gains k_i^f, k_i^b, b_i with the stipulation $k_i^f = k^f(x)|_{x=(N-i)/N}$, $k_i^b = k^b(x)|_{x=(N-i)/N}$, $b_i = b(x)|_{x=(N-i)/N}$.

We refer the reader to [1] for the details of the derivation of the PDE. The PDE model (7)-(8) is an approximation of the coupled-ODE model (5) in the sense that a finite difference discretization of the PDE yields (5).

B. Main results

We first formally define symmetric control and stability margin before stating the main results.

Definition 1: The control law (2) is *symmetric* if each agent uses the same front and back position gains: $k_i^f = k_i^b$, for all $i \in \{1, 2, \cdots, N-1\}$, and is called *homogeneous* if $k_i^f = k_j^f$, $k_i^b = k_j^b$ and $b_i = b_j$ for every pair (i, j). □

It was shown in [1] that the stability margin can be improved by a large amount by introducing front-back asymmetry in the position feedback gains. Moreover, heterogeneity has little effect on the stability margin [13]. Therefore, we consider the following asymmetric and homogeneous control gains:

$$k_i^f = (1+\epsilon)k_0, \qquad k_i^b = (1-\epsilon)k_0, \qquad b_i = b_0, \tag{9}$$

where $k_0 > 0, b_0 > 0$ are the nominal position and velocity gains respectively, and $\epsilon \in [0, 1)$ denotes the amount of asymmetry. Note that they correspond to the symmetric control gains when $\epsilon = 0$. With the control gains given in (9), it's straightforward to see that the state matrix A can be expressed in the following form,

$$A = I_N \otimes A_1 + L_g \otimes A_2, \tag{10}$$

where I_N is the $N \times N$ identity matrix and $\otimes$ is the Kronecker product. The matrices A_1, A_2 are defined as below

$$A_1 := \begin{bmatrix} 0 & 1 \\ 0 & -b_0 \end{bmatrix}, \quad A_2 := \begin{bmatrix} 0 & 0 \\ -k_0 & 0 \end{bmatrix}, \tag{11}$$

and L_g is the *directed grounded Laplacian* of the flock (see Section III):

$$L_g = \begin{bmatrix} 2 & -1+\epsilon & & & \\ -1-\epsilon & 2 & -1+\epsilon & & \\ & \cdots & \cdots & & \\ & -1-\epsilon & 2 & -1+\epsilon & \\ & & -1-\epsilon & 1+\epsilon & \end{bmatrix}. \tag{12}$$

For the PDE model, the corresponding control gains are $k^f(x) = k_0(1+\epsilon)$, $k^b(x) = k_0(1-\epsilon)$ and $b(x) = b_0$, and the PDE model is simplified to

$$\frac{\partial^2 \tilde{p}(x,t)}{\partial t^2} + b_0 \frac{\partial \tilde{p}(x,t)}{\partial t} = \frac{2\epsilon k_0}{N} \frac{\partial \tilde{p}(x,t)}{\partial x} + \frac{k_0}{N^2} \frac{\partial^2 \tilde{p}(x,t)}{\partial x^2}, \tag{13}$$

To define stability margin of the resulting PDE model (13), we take Laplace transform of both sides with respect to the time variable t and use the method of separation of variables, we have the following characteristic equation for the PDE model (refer to Section IV for more details)

$$s^2 + b_0 s + k_0 \lambda_\ell = 0, \quad \ell \in \{1, 2, \cdots\}, \tag{14}$$

where the eigenpairs $(\lambda_\ell, \phi_\ell(x))$ solve the following boundary value problem

$$\begin{aligned} \frac{d^2\phi_\ell(x)}{dx^2} + 2\epsilon N \frac{d\phi_\ell(x)}{dx} + \lambda_\ell N^2 \phi_\ell(x) = 0, \\ \frac{d\phi_\ell}{dx}(0) = 0, \quad \phi_\ell(1) = 0. \end{aligned} \tag{15}$$

For each $\ell \in \{1, 2, \cdots\}$, the two roots of the characteristic equations are denoted by $s_\ell^\pm$. The one that is closer to the imaginary axis is denoted by s_ℓ^+, and is called the *less stable* eigenvalue between the two. The set $\cup_\ell s_\ell^\pm$ constitute the eigenvalues of the PDE (13). The *least stable* eigenvalue among them is denoted by $s_{\min}$.

Definition 2: The *stability margin* of the coupled-ODE model (5), denoted by S_o, is defined as the absolute value of the real part of the least stable eigenvalue of A. The *stability margin* of the PDE model (13)-(8), denoted by S_p, is defined as the absolute value of the real part of the least stable eigenvalue of the PDE, i.e., $S_p := |Re(s_{\min})|$. □

The following theorem summaries the results in [1].

Theorem 1 (Corollary 1 and Corollary 3 of [1]): Consider an N-agent flock with PDE model (7) and boundary condition (8).

1) With symmetric and homogeneous control ($\epsilon = 0$), the stability margin S_p of flock is $S_p = O(\frac{1}{N^2})$.
2) When $0 < \epsilon \ll 1$, the optimal control gains are given by $k^f(x) = k_0(1+\epsilon)$, $k^b(x) = k_0(1-\epsilon)$ and $b(x) = b_0$, the resulting stability margin S_p of the flock is $S_p = O(\frac{\epsilon}{N})$. [1] □

Theorem 1 shows that with symmetric control, the stability margin decays to 0 as $O(1/N^2)$, irrespective of how the control gains k_0 and b_0 are chosen (as long as they are constants independent of N). The reason why we have the $O(1/N^2)$ scaling trend is because that with symmetric control the coefficient of the $\frac{\partial^2}{\partial x^2}$ term in the PDE (7) is $O(\frac{1}{N^2})$ and the coefficient of the $\frac{\partial}{\partial x}$ term is 0. However, any asymmetry between the forward and the backward position gains will lead to non-zero $k^f(x) - k^b(x)$ and a presence of $O(\frac{1}{N})$ term as the coefficient of $\frac{\partial}{\partial x}$. By a judicious choice of asymmetry, there is thus a potential to improve the stability margin from $O(\frac{1}{N^2})$ to $O(\frac{1}{N})$. Theorem 1 shows that this can indeed be achieved in the limit of $\epsilon \to 0$. Note that the coupled ODE-model provides no such insight into the effect of asymmetric control gains on the stability margin.

In this paper, we eliminate the restriction that ϵ being vanishingly small and establish the results for arbitrary but fixed ϵ. The following theorems are the main results of this section, whose proof and numerical corroboration are given in Section III and Section IV respectively. The first theorem is on the stability margin of the PDE model, and the second is on that of the original coupled-ODE model.

Theorem 2: Consider a flock with PDE model (13) and boundary condition (8). For any fixed $\epsilon \in (0,\ 1)$, the stability margin S_p is uniformly bounded from below, and is given by:

$$S_p \geq \frac{b_0 - \sqrt{b_0^2 - 4k_0\epsilon^2}}{2} = O(1). \qquad \square$$

[1]The case considered in [1] was that the optimal control gains are searched in the domain of $|k^f(x) - k_0| < \epsilon$, $|k^b(x) - k_0| < \epsilon$. It is straightforward, however, to re-derive the results if the constraints on the gains are changed to the form used here: $|k^f(x) - k_0|/k_0 < \epsilon$, $|k^b(x) - k_0|/k_0 < \epsilon$. In this paper we consider the latter case since it makes the analysis cleaner without changing the results of [1] significantly.

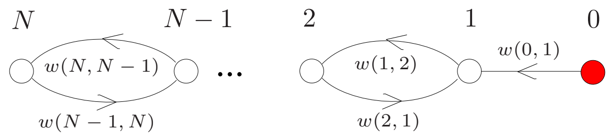

Fig. 2. Information graph for the 1-D flock of N agents and 1 reference agent. With the asymmetric control gains studied here, $w(i,i+1) = 1+\epsilon, w(i+1,i) = 1-\epsilon$.

Theorem 3: With the control gains given in (9) and for any fixed $\epsilon \in (0,\ 1)$, the stability margin S_o of the coupled-ODE model (5) is uniformly bounded from below, and is given by:

$$S_o \geq \frac{b_0 - \sqrt{b_0^2 - 8k_0(1-\sqrt{1-\epsilon^2})}}{2} = O(1). \qquad \square$$

Remark 1: Comparing the results above to the conclusions of [1] that are summarized in Theorem 1, we observe that even with an arbitrarily (but fixed and non-vanishing) amount of asymmetry, the stability margin of the system can be bounded away from zero *uniformly in* N. This asymmetric design therefore makes the resulting control law highly scalable; it eliminates the degradation of closed-loop performance with increasing N. We note that although the control law is the same as that analyzed in [1], the stronger conclusion we obtained - compared to that in [1] - is due to the fact that our analysis does not rely on a perturbation-based technique that was used [1], which limited the analysis in [1] to vanishingly small ϵ.

In addition, comparison of Theorems 2 and 3 also provide us with a quantitative measure of the error introduced in approximating the flock dynamics with a PDE. More details on the approximation error is provided in Section IV-A. $\square$

III. Stability Margin of the Coupled-ODE Model of Flock Dynamics

In this section, we provide a proof of Theorem 3. The analysis of the eigenvalues of the state matrix A relies on the spectrum of the *directed grounded Laplacian* of the flock. Before we proceed further, we formally define the information graph for the flock.

Definition 3: An *information graph* is a weighted digraph $\mathbf{G} = (\mathbf{V}, \mathbf{E})$, which associates a weight $w(i,j)$ with every edge $(i,j) \in \mathbf{E}$ in the graph. The set of edges $\mathbf{E} \subset \mathbf{V} \times \mathbf{V}$ determines the information flow and specify which pairs of nodes (agents) are allowed to exchange information to compute their local control actions. Two nodes i and j are called *neighbors* if $(i,j) \in \mathbf{E}$. $\square$

Figure 2 depicts the information graph for the 1-D flock. In our case, with the control gains given in (9), we assign the weight $1+\epsilon$ to the information from its front neighbor and $1-\epsilon$ to the information from its back neighbor. For example, for node 1, the weights we assigned to its associated edges $(0,1), (2,1)$ are $1+\epsilon$ and $1-\epsilon$ respectively.

To precisely define the *directed grounded Laplacian* L_g of the flock, recall that the *Laplacian* matrix of a graph $\mathbf{G} = (\mathbf{V}, \mathbf{E})$ with n nodes is defined as

$$[L_{N\times N}]_{ij} = \begin{cases} \sum_{k=1}^{N} w(i,k) & i=j, (i,k) \in \mathbf{E}, \\ -w(i,j) & i \neq j, (i,j) \in \mathbf{E}, \\ 0 & \text{otherwise.} \end{cases} \qquad (16)$$

The *directed grounded Laplacian* L_g matrix of $\mathbf{G}$ with respect to a set of grounded nodes $\mathbf{V}_g \subset \mathbf{V}$ is the submatrix of L obtained by removing from L those rows and columns corresponding to the grounded nodes $\mathbf{V}_g$ in $\mathbf{V}$, where $\mathbf{V}_g$ here is the node corresponding to the reference agent. The directed grounded Laplacian of the 1-D flock L_g is given in (12).

We now present a formula for the stability margin of the flock in terms of the smallest eigenvalue of its directed grounded Laplacian.

Lemma 1: With the control gains given in (9) and $0 < \epsilon < 1$, the stability margin of the flock S_o with coupled-ODE model (5) is given by

$$S_o = \begin{cases} \frac{b_0}{2}, & \text{if } \lambda_1 \geq 4k_0/b_0^2, \\ \frac{b_0 - \sqrt{b_0^2 - 4k_0\lambda_1}}{2}, & \text{otherwise.} \end{cases} \qquad (17)$$

where λ_1 is the smallest eigenvalue of the directed grounded Laplacian L_g. $\square$

Proof 1 (Proof of Lemma 1): Our proof follows a similar line of attack as of [10, Theorem 4.2]. From Schur's triangularization theorem, every square matrix is unitarily similar to an upper-triangular matrix. Therefore, there exists an unitary matrix U such that

$$U^{-1} L_g U = L_u,$$

where L_u is an upper-triangular matrix, whose diagonal entries are the eigenvalues of L_g. We now do a similarity transformation on matrix A.

$$\begin{aligned} \bar{A} :=& (U^{-1} \otimes I_2) A (U \otimes I_2) \\ =& (U^{-1} \otimes I_2)(I_N \otimes A_1 + L_g \otimes A_2)(U \otimes I_2) \\ =& I_N \otimes A_1 + L_u \otimes A_2. \end{aligned}$$

The above is a block upper-triangular matrix, and the block on each diagonal is $A_1 + \lambda_\ell A_2$, where $\lambda_\ell \in \sigma(L_g)$, where $\sigma(\cdot)$ denotes the spectrum (the set of eigenvalues). Since similarity preserves eigenvalues, and the eigenvalues of a block upper-triangular matrix are the union of eigenvalues of each block on the diagonal, we have

$$\begin{aligned} \sigma(A) = \sigma(\bar{A}) &= \bigcup_{\lambda_\ell \in \sigma(L_g)} \{\sigma(A_1 + \lambda_\ell A_2)\} \\ &= \bigcup_{\lambda_\ell \in \sigma(L_g)} \left\{ \sigma \begin{bmatrix} 0 & 1 \\ -k_0\lambda_\ell & -b_0 \end{bmatrix} \right\}. \end{aligned} \qquad (18)$$

It follows now that the eigenvalues of A are the roots s of the following characteristic equation

$$s^2 + b_0 s + k_0 \lambda_\ell = 0. \qquad (19)$$

For each $\ell \in \{1, 2, \cdots, N\}$, the two roots of the characteristic equation are denoted by $s_\ell^\pm$,

$$s_\ell^\pm = \frac{-b_0 \pm \sqrt{b_0^2 - 4k_0\lambda_\ell}}{2}. \tag{20}$$

The *least stable* eigenvalue is the one closet to the imaginary axis among them, it is denoted by $s_{\min}$. It follows from Definition 2 that $S_o = |Re(s_{\min})|$.

Depending on the discriminant in (20), there are two cases to analyze:

(1) If $\lambda_1 \geq 4k_0/b_0^2$, then the discriminant in (20) for each ℓ is non-positive, which yields

$$S_o = |Re(s_{\min})| = \frac{b_0}{2}.$$

(2) Otherwise, the less stable eigenvalue can be written as

$$s_\ell^+ = \frac{-b_0 + \sqrt{b_0^2 - 4k_0\lambda_\ell}}{2}.$$

The least stable eigenvalue is obtained by setting $\lambda_\ell = \lambda_1$, so that

$$S_o = |Re(s_{\min})| = \frac{b_0 - \sqrt{b_0^2 - 4k_0\lambda_1}}{2}. \qquad \blacksquare$$

We are now ready to present the proof of Theorem 3.

Proof 2 (Proof of Theorem 3): From Lemma 1, we see that the smallest eigenvalue of the directed grounded Laplacian plays an important role in determining the stability margin of the 1-D flock. To get an lower bound of the stability margin, a lower bound for the smallest eigenvalue is needed. For the general asymmetric case ($0 < \epsilon < 1$), it follows from Eq. (6)-(7) of [14] that the eigenvalues of L_g, denoted by λ_ℓ, are given by

$$\lambda_\ell = 2 - 2\sqrt{1-\epsilon^2}\cos\theta_\ell, \quad \ell \in \{1, 2, \cdots, N\}, \tag{21}$$

where θ_ℓ is the ℓ-th root of the following equation

$$\sqrt{\frac{1+\epsilon}{1-\epsilon}}\sin(N+1)\theta = \sin N\theta, \tag{22}$$

where $\theta \neq m\pi, m \in \mathbb{Z}$, the set of integers. From formula (21), we see that the eigenvalues of L_g are real and positive, and moreover, $0 < \lambda_1 < \lambda_2 < \cdots < \lambda_N$. To see why, first notice that we only need consider the roots of (22) in the open interval $(0, 2\pi)$, in which there are $2N$ nontrivial isolated roots, see Figure 3 for an example. The roots located in $\mathbb{R} \setminus (0, 2\pi)$ are just $2m\pi$ ($m \in \mathbb{Z}$) distance away from those in $(0, 2\pi)$. Moreover, if $\theta_0 \in (0, 2\pi)$ is a solution of (22), then $2\pi - \theta_0$ is also a solution. Therefore, we can restrict the domain of analysis to $(0, \pi)$, in which there are N isolated roots. The ordering of the eigenvalues follows from $\cos\theta$ being a decreasing function in $(0, \pi)$.

It also follows that θ_1, the smallest positive root of (22), leads to the smallest eigenvalue. It is straightforward to show that the ℓ-th root θ_ℓ is in the open interval $(\frac{(2\ell-1)\pi}{2(N+1)}, \frac{(2\ell+1)\pi}{2(N+1)})$. Now, the smallest eigenvalue of the directed grounded Laplacian L_g is given by

$$\lambda_1 = 2 - 2\sqrt{1-\epsilon^2}\cos\theta_1, \tag{23}$$

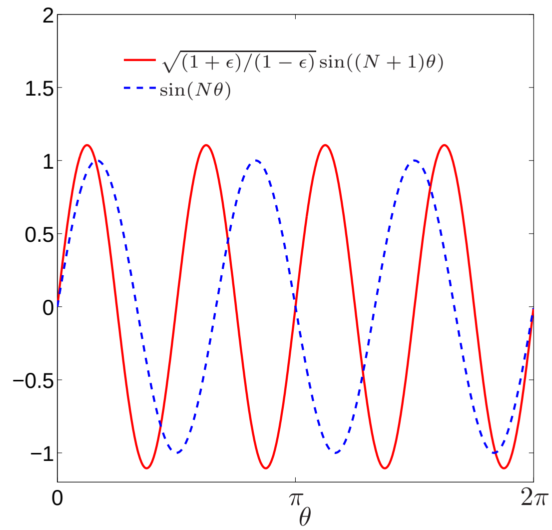

Fig. 3. Graphical solution θ of $\sqrt{(1+\epsilon)/(1-\epsilon)}\sin((N+1)\theta) = \sin(N\theta)$ with $\epsilon = 0.1$ and $N = 3$.

where $\theta_1 \in (\frac{\pi}{2(N+1)}, \frac{3\pi}{2(N+1)})$. Take the limit $N \to \infty$, we have the following infimum for the smallest eigenvalue:

$$\inf_N \lambda_1 = 2 - 2\sqrt{1-\epsilon^2}. \tag{24}$$

To prove Theorem 3, we consider the following two cases: (1) Case 1: $\lambda_1 \geq 4k_0/b_0^2$. According to Lemma 1, the stability margin is given by $S_o = b_0/2$. (2) Case 2: $\lambda_1 < 4k_0/b_0^2$. From Lemma 1, the stability margin is given by

$$S_o = \frac{b_0 - \sqrt{b_0^2 - 4k_0\lambda_1}}{2}.$$

Since $\lambda_1 \geq 2 - 2\sqrt{1-\epsilon^2}$, the stability margin for this case is bounded below

$$S_o \geq \frac{b_0 - \sqrt{b_0^2 - 8k_0(1 - \sqrt{1-\epsilon^2})}}{2}. \tag{25}$$

Notice that the above lower bound (25) is smaller than $b_0/2$ (value of S_o in case 1), we complete the proof. $\blacksquare$

A. Numerical comparisons

In this section, we present the numerical comparison results between the stability margins of the flock with symmetric control (Theorem 1) and with asymmetric control (Theorem 3). The stability margins are obtained by numerically evaluating the eigenvalues of the state matrix A. Figure 4 depicts the comparison results between the stability margins for the two cases: symmetric and asymmetric controls. The nominal control gains used are $k_0 = 1$, $b_0 = 0.5$, and for asymmetric control, the amount of asymmetry used is $\epsilon = 0.1$.[2] We note that for asymmetric control, the control

[2]When ϵ is large, numerical errors in eigenvalue computations arise when the dimension of the matrix A is large. This is observed by numerically comparing the eigenvalues of the matrix with those of a random similarity transformation of the matrix, which in MATLAB© produces distinct results.

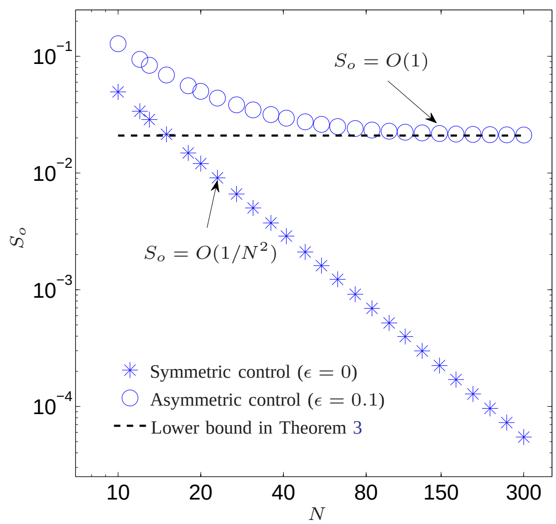

Fig. 4. Stability margin comparisons between the flock with symmetric control and asymmetric control.

gains satisfy the second case of Lemma 1, so that the Theorem 3 predicts that the stability margin is bounded below by $(b_0 - \sqrt{b_0^2 - 8k_0(1-\sqrt{1-\epsilon^2})}/2 \approx 0.0209$. We can see from Figure 4 that the stability margin of the flock with asymmetric control is indeed bounded away from 0 uniformly in N, and the prediction of the theorem is quite accurate. Furthermore the stability margin with asymmetric control is much larger than that with symmetric control.

IV. Stability Margin of the PDE Approximation of Flock Dynamics

In this section, we present the stability margin of the flock with PDE model (13) and boundary condition (8). Since the PDE model (13) and boundary condition (8) are linear and homogeneous, we are able to apply the method of separation of variables. We assume a solution of the form $\tilde{p}(x,t) = \sum_{\ell=1}^{\infty} \phi_\ell(x) h_\ell(t)$. Substituting it into PDE (13), we obtain the following time-domain ODE

$$\frac{d^2 h_\ell(t)}{dt^2} + b_0 \frac{dh_\ell(t)}{dt} + k_0 \mu_\ell h_\ell(t) = 0, \tag{26}$$

where μ_ℓ solves the following boundary value problem

$$\mathcal{L}\phi_\ell(x) = 0, \quad \mathcal{L} := \frac{d^2}{dx^2} + 2\epsilon N \frac{d}{dx} + \mu_\ell N^2, \tag{27}$$

with the following boundary condition, which comes from (8):

$$\frac{d\phi_\ell}{dx}(0) = 0, \quad \phi_\ell(1) = 0. \tag{28}$$

Taking Laplace transform of both sides of (26) with respect to the time variable t, we have the following characteristic equation for the PDE model

$$s^2 + b_0 s + k_0 \mu_\ell = 0. \tag{29}$$

To prove Theorem 2, we need the following lemma.

Lemma 2: The eigenvalues μ_ℓ ($\ell \in \{1, 2, \cdots\}$) of the Strum-Liouville operator $\mathcal{L}$ with boundary condition (28) for $0 < \epsilon < 1$ are real and satisfy

$$\mu_\ell = \epsilon^2 + \frac{a_\ell^2}{N^2}, \tag{30}$$

where a_ℓ is the root of $-a_\ell/(\epsilon N) = \tan(a_\ell)$, and in particular, $a_\ell \in (\frac{(2\ell-1)\pi}{2}, \ell\pi)$. □

Proof 3 (Proof of Lemma 2): We first multiply both sides of (27) by $e^{2\epsilon N x} N^2$, we obtain the standard Sturm-Liouville eigenvalue problem

$$\frac{d}{dx}\left(e^{2\epsilon N x} \frac{d\phi_\ell(x)}{dx}\right) + \mu_\ell^{(\epsilon)} N^2 e^{2\epsilon N x} \phi_\ell(x) = 0. \tag{31}$$

According to Sturm-Liouville Theory, all the eigenvalues are real and have the following ordering $\mu_1 < \mu_2 < \cdots$, see [15]. To solve the boundary value problem (27)-(28), we assume solution of the form, $\phi_\ell(x) = e^{rx}$, then we obtain the following equation

$$\begin{aligned} r^2 + 2\epsilon N r + \mu_\ell N^2 = 0, \\ \Rightarrow r = -\epsilon N \pm N\sqrt{\epsilon^2 - \mu_\ell}. \end{aligned} \tag{32}$$

Depending on the discriminant in the above equation, there are three cases to analyze:

1) $\mu_\ell < \epsilon^2$, then the eigenfunction $\phi_\ell(x)$ has the following form $\phi_\ell(x) = c_1 e^{(-\epsilon N + N\sqrt{\epsilon^2-\mu_\ell})x} + c_2 e^{(-\epsilon N - N\sqrt{\epsilon^2-\mu_\ell})x}$, where c_1, c_2 are some constants. Applying the boundary condition (28), it's straightforward to see that, for non-trivial eigenfunctions $\phi_\ell(x)$ to exit, the following equation must be satisfied $(\epsilon N - N\sqrt{\epsilon^2-\mu_\ell})/(\epsilon N + N\sqrt{\epsilon^2-\mu_\ell}) = e^{2N\sqrt{\epsilon^2-\mu_\ell}}$. For positive ϵ, this leads to a contradiction, so there is no eigenvalue for this case.
2) $\mu_\ell = \epsilon^2$, then the eigenfunction $\phi_\ell(x)$ has the following form
$$\phi_\ell(x) = c_1 e^{-\epsilon N x} + c_2 x e^{-\epsilon N x}.$$
Again, applying the boundary condition (28), for non-trivial eigenfunctions $\phi_\ell(x)$ to exit, we have the following $\epsilon N = -1$, which implies there is no eigenvalue for this case either.
3) $\mu_\ell > \epsilon^2$, then the eigenfunction $\phi_\ell(x)$ has the following form $\phi_\ell(x) = e^{-\epsilon N x}(c_1 \cos(N\sqrt{\mu_\ell - \epsilon^2}x) + c_2 \sin(N\sqrt{\mu_\ell - \epsilon^2}x))$. Applying the boundary condition (28), for non-trivial eigenfunctions $\phi_\ell(x)$ to exit, the eigenvalues μ_ℓ must satisfy (30) and a_ℓ solves the transcendental equation $-a_\ell/(\epsilon N) = \tan(a_\ell)$. A graphical representation of the functions $\tan x$ and $-x/\epsilon N$ with respect to x shows that $a_\ell \in (\frac{(2\ell-1)\pi}{2}, \ell\pi)$. ■

We now present the proof for Theorem 2.

Proof 4 (Proof of Theorem 2): From Lemma 2, we see that $a_1 \in (\pi/2, \pi)$, and (30) implies $\mu_1 \to \epsilon^2$ from above as $N \to \infty$, i.e. $\inf_N \mu_1 = \epsilon^2$. From the characteristic equation (29), the eigenvalues of the PDE model are given by

$$s_\ell^\pm = \frac{-b_0 \pm \sqrt{b_0^2 - 4k_0\mu_\ell}}{2}. \qquad (33)$$

Depending on the discriminant in (33), there are two cases to analyze: (1) If $\mu_1 \geq 4k_0/b_0^2$, then the discriminant in (33) for each ℓ is non-positive, which yields $S_p = |Re(s_{\min})| = b_0/2$. (2) Otherwise, the less stable eigenvalue can be written as

$$s_\ell^+ = \frac{-b_0 + \sqrt{b_0^2 - 4k_0\mu_\ell}}{2}.$$

The least stable eigenvalue is obtained by setting $\mu_\ell = \mu_1$, so that

$$S_p = |Re(s_{\min})| = \frac{b_0 - \sqrt{b_0^2 - 4k_0\mu_1}}{2} \geq \frac{b_0 - \sqrt{b_0^2 - 4k_0\epsilon^2}}{2}.$$

Again, note that the above lower bound is smaller than $b_0/2$ (value of S_p in case 1), we complete the proof. ■

A. Error analysis of the PDE approximation

We next provide an error analysis on the PDE approximation, which answers the question on how well the PDE model approximates the flock dynamics. The characteristic equation of the coupled-ODE model of the flock that leads to the least stable eigenvalue is $s^2 + b_0 s + k_0\lambda_1 = 0$, while the corresponding characteristic equation of the PDE model is $s^2 + b_0 s + k_0\mu_1 = 0$. Comparing the two, it is obvious that the error in the stability margin prediction by the PDE approximation is determined by the difference between λ_1, the smallest eigenvalue of the directed grounded Laplacian L_g, and μ_1, the smallest eigenvalue of the Sturm-Liouville operator $\mathcal{L}$. Since the PDE model is developed as an approximation of the flock in the limit $N \to \infty$, we consider the respective eigenvalues in this limit. Specifically, define $\bar{\lambda}_1 := \lim_{N\to\infty} \lambda_1$ and $\bar{\mu}_1 = \lim_{N\to\infty} \mu_1$. The following lemma quantifies the difference between $\bar{\mu}_1$ and $\bar{\lambda}_1$, whose proof follows in a straightforward manner from (24) and (30).

Lemma 3: The difference between the smallest eigenvalues of the directed grounded Laplacian L_g and the Sturm-Liouville operator $\mathcal{L}$ is asymptotically

$$\bar{\lambda}_1 - \bar{\mu}_1 = 2 - 2\sqrt{1-\epsilon^2} - \epsilon^2 = \frac{1}{4}\epsilon^4 + O(\epsilon^6), \qquad (34)$$

where the formula holds for arbitrary $\epsilon \in [0, 1)$. □

Figure 5 shows numerical comparisons between the smallest eigenvalue of the directed grounded Laplacian L_g with that of the Sturm-Liouville operator $\mathcal{L}$ for different amounts of asymmetry. The eigenvalues of the directed grounded Laplacian are obtained by using the prediction (21)-(22). [3] For the Sturm-Liouville operator $\mathcal{L}$, we use formulae (30), which involves numerically solving the associated transcendental equation $-a_\ell/(\epsilon N) = \tan(a_\ell)$ to compute its

[3]Direct eigenvalue computation in MATLAB© works only for small ϵ. When the value of ϵ is larger than 0.2, MATLAB© produces erroneous results, since the eigenvalues of L_g and those of a random similarity transformation computed by MATLAB© are seen to be different.

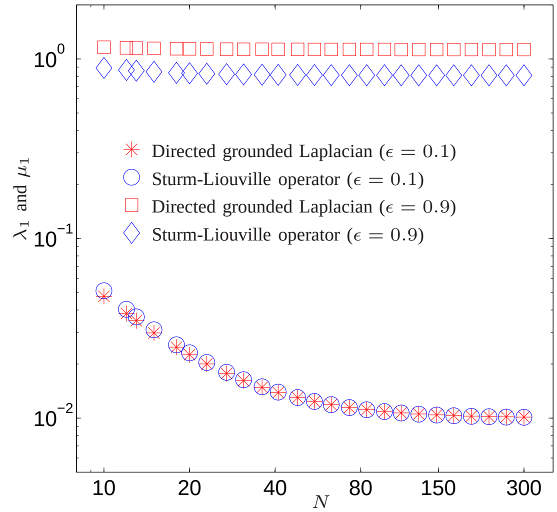

Fig. 5. Numerical comparisons between the smallest eigenvalue of the directed grounded Laplacian, λ_1, and that of the Sturm-Liouville operator, μ_1. The difference between λ_1 and μ_1 is negligible for small ϵ (even for small N), but noticeable for large ϵ.

eigenvalues. The amounts of asymmetry used are $\epsilon = 0.1$ and $\epsilon = 0.9$ respectively. We plot the smallest eigenvalues of the directed grounded Laplacian and the Sturm-Liouville operator as a function of N, the number of agents in the flock. From Figure 5, we can see that for small amount of asymmetry $\epsilon = 0.1$, the smallest eigenvalue of the Sturm-Liouville operator matches that of the directed grounded Laplacian very well, especially when N is large. However, for large amount of asymmetry $\epsilon = 0.9$, the difference between the smallest eigenvalues is not negligible anymore.

The next result describes the stability margin approximation error introduced by the PDE model due to the control asymmetry.

Theorem 4: The difference between the predictions of the stability margin of the flock by the coupled-ODE model (5) and the PDE model (13)-(8) is, asymptotically,

$$S_o - S_p = \begin{cases} 0, & \text{if } \frac{b_0^2}{4k_0} \leq \epsilon^2, \\ \frac{b_0}{2}\left(1 - \frac{2k_0\epsilon^2}{b_0^2}\right) + O(\epsilon^4) & \text{if } \epsilon^2 < \frac{b_0^2}{4k_0} \leq 2 - 2\sqrt{1-\epsilon^2} \\ \frac{k_0}{4b_0}\epsilon^4 + O(\epsilon^6) & \text{if } 2 - 2\sqrt{1-\epsilon^2} < \frac{b_0^2}{4k_0} \end{cases}$$

where asymptotically means the formula holds for $N \to \infty$. □

Proof 5 (Proof of Theorem 4): For future use, define $\alpha := \frac{b_0^2}{4k_0}$. It follows from the discussion preceding Lemma 3 that the relevant roots of the characteristic equations for the coupled-ODE and PDE models are $\frac{1}{2}b_0\left(-1 + (1 - \bar{\lambda}_1/\alpha)^{1/2}\right)$ and $\frac{1}{2}b_0\left(-1 + (1 - \bar{\mu}_1/\alpha)^{1/2}\right)$, respectively. It follows from Lemma 3 that $2(1 - \sqrt{1-\epsilon^2}) = \bar{\lambda}_1 > \bar{\mu}_1 = \epsilon^2$. Hence, we have three cases to consider: (i) $\alpha \leq \bar{\mu}_1$, (ii) $\bar{\mu}_1 < \alpha \leq \bar{\lambda}_1$, and (iii) $\bar{\lambda}_1 < \alpha$. For convenience of asymptotic analysis, we first define $\bar{S}_o := \lim_{N\to\infty} S_o$ and $\bar{S}_p := \lim_{N\to\infty} S_p$.

1) $\alpha \leq \epsilon^2 = \bar{\mu}_1 (< \bar{\lambda}_1)$: In this case, the real parts of the least stable eigenvalues for both the coupled-ODE and PDE models are $-b_0/2$. Hence $\bar{S}_o - \bar{S}_p = 0$.
2) $\epsilon^2 < \alpha \leq \bar{\lambda}_1$: In this case the discriminant in the coupled-ODE model's least stable eigenvalue is zero or negative, so that $\bar{S}_o = b_0/2$, while the discriminant in the PDE model's least stable eigenvalue is positive, which makes it real. In this case it is straightforward to show that

$$\begin{aligned}\bar{S}_o - \bar{S}_p &= \frac{1}{2} b_0 (1 - \bar{\mu}_1/\alpha)^{1/2} = \frac{1}{2} b_0 (1 - \frac{\epsilon^2}{2\alpha}) + O(\epsilon^4) \\ &= \frac{b_0}{2} (1 - \frac{2k_0\epsilon^2}{b_0^2}) + O(\epsilon^4).\end{aligned}$$

3) $\bar{\lambda}_1 < \alpha$: In this case both $\bar{S}_p$ and $\bar{S}_o$ are real, and their values are given by the infima in Theorems 2 and 3. The difference between them is

$$\begin{aligned}\bar{S}_o - \bar{S}_p &= \frac{b_0}{2}\Big((1 - \frac{\epsilon^2}{\alpha})^{1/2} - (1 - \frac{2 - 2\sqrt{1-\epsilon^2}}{\alpha})^{1/2}\Big) \\ &= \frac{b_0}{2}\Big(\frac{\epsilon^4}{8\alpha} + O(\epsilon^6)\Big) = \frac{k_0}{4b_0}\epsilon^4 + O(\epsilon^6),\end{aligned}$$

where the second equality follows upon using Taylor series expansions.

The results in the theorem follows upon noting that $\bar{S}_o$, $\bar{S}_p$ are asymptotic values of S_o and S_p. ■

Remark 2: It may seem from above that the "approximation error" (the error in the stability margin prediction by the PDE approximation) is minimized for case (i), when $\epsilon^2 \geq \frac{b_0^2}{4k_0}$. However, this is due to the fact that the stability margin only depends on the real part of the eigenvalues. In case (i), it is possible that the least stable eigenvalue predicted by the PDE approximation is quite different from that of the ODE model, due to the difference in the imaginary part. In fact, the error in the prediction of the least stable eigenvalue by the PDE model is smallest in case (iii), when both the ODE and PDE eigenvalues are real. In case (iii), we see that if the amount of asymmetry $0 < \epsilon \ll 1$, then the approximation error is $O(\epsilon^4)$ for large N. Thus, the error introduced by the PDE approximation is negligible for small amounts of asymmetry. However, when the amount of asymmetry is large, the PDE approximation has a non-negligible error. □

V. Summary

We studied the stability margin of a large 1-D flock of double-integrator agents. The control is decentralized: the control signal at every agent depends on the relative measurements from its nearest neighbors. Inspired by the previous works [1], [6], we examined the role of asymmetry in the control gains on the stability margin of the flock. We showed that with any fixed amount of asymmetry in the control gains, the stability margin of the 1-D flock can be bounded away from 0, uniformly in N. This eliminates the problem of loss of stability margin with increasing N that is seen with symmetric control. In this paper, the analysis of the stability margin avoids the perturbation method used in [1], [6], which limited the analyses in those papers to vanishingly small amount of asymmetry. We also provide an error bound on the stability margin predicted by the PDE approximation.

It is noteworthy that heterogeneity in control gains and agent dynamics has little effect on the stability margin [13] and sensitivity to disturbances [16], while asymmetry has a significant impact, as we showed here. In this paper we do not examine the issue of disturbance propagation, though numerical evidence suggests asymmetry also reduces the sensitivity to external disturbances; see [1], [17]. This topic is a subject of ongoing research.

References

[1] P. Barooah, P. G. Mehta, and J. P. Hespanha, "Mistuning-based decentralized control of vehicular platoons for improved closed loop stability," *IEEE Transactions on Automatic Control*, vol. 54, no. 9, pp. 2100–2113, September 2009.

[2] J. K. Hedrick, M. Tomizuka, and P. Varaiya, "Control issues in automated highway systems," *IEEE Control Systems Magazine*, vol. 14, pp. 21 – 32, December 1994.

[3] R. Olfati-Saber, J. Fax, and R. Murray, "Consensus and cooperation in networked multi-agent systems," *Proceedings of the IEEE*, vol. 95, no. 1, pp. 215–233, 2007.

[4] E. Wagner, D. Jacques, W. Blake, and M. Pachter, "Flight test results of close formation flight for fuel savings," in *AIAA Atmospheric Flight Mechanics Conference and Exhibit*, 2002, AIAA-2002-4490.

[5] H. Tanner and D. Christodoulakis, "Decentralized cooperative control of heterogeneous vehicle groups," *Robotics and autonomous systems*, vol. 55, no. 11, pp. 811–823, 2007.

[6] H. Hao, P. Barooah, and P. G. Mehta, "Stability margin scaling of distributed formation control as a function of network structure," *to appear, IEEE Transactions on Automatic Control*, April 2011. [Online]. Available: http://plaza.ufl.edu/hehao/publication.html

[7] P. Seiler, A. Pant, and J. K. Hedrick, "Disturbance propagation in vehicle strings," *IEEE Transactions on Automatic Control*, vol. 49, pp. 1835–1841, October 2004.

[8] B. Bamieh, M. R. Jovanović, P. Mitra, and S. Patterson, "Effect of topological dimension on rigidity of vehicle formations: fundamental limitations of local feedback," in *Proceedings of the 47th IEEE Conference on Decision and Control*, Cancun, Mexico, 2008, pp. 369–374.

[9] M. R. Jovanović and B. Bamieh, "On the ill-posedness of certain vehicular platoon control problems," *IEEE Trans. Automat. Control*, vol. 50, no. 9, pp. 1307–1321, September 2005.

[10] J. Veerman, "Stability of large flocks: an example," July 2009, arXiv:1002.0768.

[11] J. Veerman, B. Stošić, and F. Tangerman, "Automated traffic and the finite size resonance," *Journal of Statistical Physics*, vol. 137, no. 1, pp. 189–203, October 2009.

[12] P. Chebotarev and R. Agaev, "Coordination in multiagent systems and laplacian spectra of digraphs," *Automation and Remote Control*, vol. 70, no. 3, pp. 469–483, 2009.

[13] H. Hao and P. Barooah, "Control of large 1d networks of double integrator agents: role of heterogeneity and asymmetry on stability margin," in *IEEE Conference on Decision and Control*, December 2010.

[14] W. Yueh, "Eigenvalues of several tridiagonal matrices," *Applied Mathematics E-Notes*, vol. 5, pp. 66–74, 2005.

[15] R. Haberman, *Elementary applied partial differential equations: with Fourier series and boundary value problems*. Prentice-Hall, 2003.

[16] R. Middleton and J. Braslavsky, "String instability in classes of linear time invariant formation control with limited communication range," *Automatic Control, IEEE Transactions on*, vol. 55, no. 7, pp. 1519–1530, 2010.

[17] H. Hao, P. Barooah, and P. Mehta, "Stability Margin Scaling Laws for Distributed Formation Control as a Function of Network Structure," *Arxiv preprint arXiv:1005.0351*, 2010.